WESTINGHOUSE PROPRIETARY CLASS 3

WCAP-8860-S2

MASS AND ENERGY RELEASES FOLLOWING

A STEAM LINE RUPTURE

SUPPLEMENT 2 - IMPACT OF STEAM SUPERHEAT IN MASS/ENERGY RELEASES FOLLOWING A STEAMLINE RUPTURE FOR DRY AND SUBATMOSPHERIC CONTAINMENT DESIGNS

September 1985

AUTHORS

J. C. Butler
P. A. Linn

WESTINGHOUSE ELECTRIC CORPORATION
NUCLEAR ENERGY SYSTEMS
P. O. BOX 355
PITTSBURGH, PENNSYLVANIA 15230

IMPACT OF STEAM SUPERHEAT IN MASS/ENERGY RELEASES
FOLLOWING A STEAMLINE RUPTURE
FOR DRY AND SUBATMOSPHERIC CONTAINMENT DESIGNS

LIST OF TABLES

LIST OF FIGURES

LIST OF FIGURES (Continued)

I. INTRODUCTION

During the NRC Containment Systems Branch review of the Westinghouse topical report, "Mass and Energy Releases Following a Steamline Rupture", WCAP-8822 (Reference 1), the Staff noted that heat transfer to steam from the uncovered portion of the steam generator tube bundle was unaccounted for and questioned the effect of steam superheating upon the mass/energy release and the subsequent effect on the containment temperature response. Westinghouse responded in a letter to the Staff in February 1982 (Reference 2) that it had determined the impact of the effect by conservatively treating the maximum amount of superheat to be the difference between the primary coolant temperature and the steam temperature. The letter noted that dry containments would exibit [ ]^{a,c} to superheat in the blowdowns.

Since that time, Westinghouse has performed additional steamline break analyses to reconfirm the conclusion reached in Reference 2 for dry containments and to extend the analyses to include subatmospheric containment designs. This report describes these analyses and is provided as a second supplement to WCAP-8822.

II. STEAMLINE BREAK CALCULATIONAL MODEL

A. Mass/Energy Release Model

The methodology which is currently used by Westinghouse in the analysis of steamline break mass and energy releases for dry and subatmospheric containment designs is based upon information presented in the following reports:

- WCAP-8822, "Mass and Energy Releases Following a Steam Line Rupture" (Reference 1),

- WCAP-7907-P-A, "LOFTRAN Code Description" (Reference 5),

- WCAP-8326, "Containment Pressure Analysis Code (COCO)" (Reference 7).

WCAP-8822 forms the basis for assumptions and models used in the calculation of the mass and energy releases resulting from a steam line rupture. WCAP-8822 presents an extensive analysis of the nature of effluent releases from Westinghouse steam generators following a postulated main steam line rupture, as well as a discussion of the methods and models used.

WCAP-7907 documents the LOFTRAN computer code. The LOFTRAN code is used to generate mass and energy releases following a steamline rupture. This information is then input into an appropriate containment code which analyzes the resultant impact on containment pressure and temperature.

LOFTRAN Computer Code

Mass and energy releases for the analyses discussed in this report were calculated using the LOFTRAN code (Reference 5). The LOFTRAN code has been used by Westinghouse for the calculation of mass/energy releases during a steamline rupture for several years and has replaced the MARVEL code (referenced in WCAP-8822) as the primary non-LOCA systems analysis code.

For all of the analyses presented in this report, a modified version of LOFTRAN was used. The modifications which were incorporated into LOFTRAN enable the modeling of steam superheating of mass/energy blowdowns during steamline breaks. A discussion of the modeling modifications to LOFTRAN is provided in Reference 6.

Base Plant Description

A typical 4 loop Westinghouse NSSS plant design was used as the base line model for all the steamline break analyses presented in this document. Basic design parameters are given in Table II-1. The following sections describe the important subsystems modeled in the LOFTRAN code.

Kinetics Modeling

The LOFTRAN code utilizes a point kinetics model to describe the core nuclear power transient initiated by the cooldown following a steamline rupture. The model includes a conservative calculation of decay heat generation and energy release from residual fissions. Values used for the required kinetics variables are given in Table II-2, and are appropriate for end-of-life core conditions in a Westinghouse 17X17 core design. For all analyses, the most reactive control rod is assumed to be stuck out of the core. The "stuck rod" assumption results in higher blowdown rates due to increased power generation in the core and also results in higher RCS fluid temperatures. Both of these effects are conservative with respect to the impact of steam superheating, as the increased blowdown results in earlier tube bundle uncovery while higher RCS temperatures result in higher steam temperatures.

Latent Energy Sources

Latent heat energy from reactor vessel and primary system piping thick metal, and reverse heat transfer from steam generators which have been isolated from the broken steam line were included in total RCS heat load. The LOFTRAN thick metal heat transfer model is described in Reference 5.

Steam Generator Heat Transfer Model

The ability of the steam generator(s) feeding the broken steam line to transfer heat from the primary coolant to the secondary water inventory has an important influence on the mass and energy that are released through the break. The film coefficient on the outside of the tubes during a blowdown will generally be due to some form of stable boiling forced by the continual depressurization of the steam generator and the addition of auxiliary feedwater. This situation will exist for long periods after the break occurs and will keep the secondary side heat transfer coefficient large. As the effective liquid level in the steam generator drops below the top of the tube bundle region, the heat transfer switches to superheated steam forced convection which results in a large reduction in the heat transfer from the RCS to the steam generator secondary side in the uncovered tube bundle region. In the analyses described in Reference 1, heat transfer to steam in the uncovered tube bundle region was not included in the steam generator heat transfer model. Neglecting heat transfer to steam (i.e., steam superheating) in the uncovered tube bundle region has little impact on the total energy transfer from primary to secondary because of the large reduction in heat transfer which occurs in the transition to forced steam convection. Not accounting for steam superheating does, however, result in an underprediction of effluent steam temperatures. For the present analyses, a modified version of LOFTRAN was used which explicitly accounts for heat transfer to steam in the uncovered portion of the tube bundle region. The models to accomplish this and their incorporation into LOFTRAN are discussed in Reference 6.

Safety System Modeling

Following a steamline rupture, many safety systems which are designed to mitigate the consequences of the accident come into operation. Among these are the steam and feedwater isolation valves, the control and shutdown rods, and the safety injection system.

Each of these systems was modeled in a conservative manner by the LOFTRAN code. For each case evaluated, appropriate assumptions pertaining to setpoints, valve operating speeds, signal and processing delays, etc. were used. Table II-3 lists these assumptions.

Feedwater System Model

To maximize the water inventory available to be released through the broken line, large values of feedwater flow were used in the LOFTRAN blowdown analyses. The feedwater flow transients used in the LOFTRAN analyses are described in Table II-4.

Auxiliary feedwater addition is simulated by assuming a [ ]^{a,c} flow to the faulted steam generator equal to [ ]^{a,c} The effects of any flashing of the feedwater trapped between the steam generator and the isolation valves is also included in the analyses.

Steam Generator Mass Inventory

[ ]^{a,c} values of initial steam generator mass corresponding to [ ]^{a,c} were used in the system blowdown transients for conservatism.

Availability of Offsite Power

The availability of offsite power was assumed in all system analyses using LOFTRAN. Specifically, no credit was taken for tripping the reactor coolant pumps in determining the steam line break mass and energy releases, since tripping of the pumps results in a significant decrease in the blowdown rate.

Blowdown and Entrainment Modeling

The blowdown quality assumptions used in the present analyses are based upon detailed entrainment calculations performed using the TRANFLO code. The TRANFLO entrainment calculations, as well as the conditions for which entrainment would be experienced, (i.e. break size, power level), are discussed in Reference 1.

B. Containment Response Model

The methodology used by Westinghouse to calculate the containment response to a postulated steamline break in dry and subatmospheric containment designs is based upon information presented in the following reports:

- WCAP-8326, "Containment Pressure Analysis Code (COCO)" (Reference 7)
- WCAP-9558, "Environmental Qualification Instrument Transmitter Temperature Transient Analysis" (Reference 4).

COCO Computer Code

The COCO code is a one node containment code used to calculate the containment pressure and temperature transient following a postulated high energy line break. COCO is a sophisticated mathematical model of a generalized dry containment. For analytical rigor, the containment steam-air-water mixture is separated into two distinct systems. The first system consists of a steam-air phase, while the second system is of the liquid water phase. Thermal equilibrium is assumed between the steam and the air. The air is treated as an ideal gas. The thermodynamic properties of water and steam are derived from compressed water and steam tables.

The COCO code can model the heat transfer to the passive heat sinks located in the containment, as well as the heat transfer to the active Containment Heat Removal Systems (i.e., the containment fan coolers and the containment sprays).

For large steamline breaks, the assumption is made that [ ]^{a,c} of the condensate formed on the passive heat sinks will be swept back into the containment atmosphere. This assumption is appropriate for large breaks due to the higher velocities induced by the break jet. For smaller breaks, the velocities will be lower and will be insufficient to sweep the condensate off of the walls. For these smaller break cases, the assumption is made that all of the condensate calculated to form on the heat sinks will fall directly to the sump without interacting with the steam-air space. WCAP-8936 (Reference 8) describes the methodology used to calculate the amount of condensate formed on the heat sink.

The methodology described in References 7 and 8, which is summarized in the preceding paragraphs, is the standard Westinghouse methodology. No changes to this methodology were required to specifically address the superheated steam exiting the steam generators.

Base Containment Parameter Description

Two containment models were used to determine the impact of the additional heat release due to the superheated steam. The first model represents a typical large dry PWR containment building and the second represents a subatmospheric containment building. Table II-5 shows specific parameters used for the first model while Table II-6 gives specific parameters for the subatmospheric model.

TABLE II-1

PLANT DESIGN PARAMETERS

Nuclear Steam Supply System	
Power (MWt)	3423
Reactor Coolant Pressure (psia)	2250
Thermal Design Flow (gpm/loop)	87,300
Vessel Average Temperature (°F)	577.9
Nominal Vessel delta T (°F)	65.8
Steam Generator Temperature (°F)	519.0
Steam Pressure (psia)	805
Steam Flow (lbm/sec/loop)	1032
Feedwater Enthalpy (BTU/lbm)	432.8
Core Design	
Fuel Type	17 X 17
Average Power Density (kw/ft)	5.33
Fuel Mass (lbm)	235637
Fuel Pin Diameter (in)	0.374
Fuel Clad Thickness (in)	0.0225
Steam Generator	
Type	Model 51
Heat Transfer Area (Ft^2)	51500.
Shell Design Pressure (psia)	1100.
Number of U-tubes	3388
Tube Height (Ft)	34.75

TABLE II-2

NUCLEAR KINETICS DATA

Parameter	Value
Effective Delayed Neutron Fraction (end-of-life)	.0044
Keff versus Temperature	See Figure II-1
Doppler Power Coefficient (Hot Zero Power)	See Figure II-2
Shutdown Margin (%)	1.6
Prompt Neutron Lifetime (microseconds)	26.

TABLE II-3

SAFETY SYSTEMS ASSUMPTIONS

Trip Setpoints	
High Nuclear Flux	118% Nominal
Low Pressurizer Pressure Reactor Trip	1775 psia
Low Pressurizer Pressure Safety Injection	1715 psia
Low Steam Line Pressure	359 psia
Safety Injection	
SI Flowrate	See Figure II-3
Boron Concentration in SI Lines	0 ppm
Boron Concentration in BIT	0 ppm
Boron Concentration in RWST	2000 ppm
Time Constants	
Steam Line Isolation Valve Closing Time	8 seconds
Feed Line Isolation Valve Closing Time	7 seconds
Steam Line Pressure Lead Time Constant	50 seconds
Steam Line Pressure Lag Time Constant	5 seconds
SI Pump Start-up Time	20 seconds

TABLE II-4

FEEDWATER FLOW ASSUMPTIONS

FOR LOFTRAN ANALYSES

MAIN FEEDWATER FLOW TO THE FAULTED STEAM GENERATOR	
LARGE DOUBLE-ENDED RUPTURES	200% NOMINAL
SMALL DOUBLE-ENDED RUPTURES	200% NOMINAL
SPLIT RUPTURES	200% NOMINAL
FEEDWATER ENTHALPY	
102% POWER	411.6 BTU/LBM
70% POWER	370.3 BTU/LBM
30% POWER	292.4 BTU/LBM
HOT SHUTDOWN	100.0 BTU/LBM
MAIN FEEDWATER FLASHING VOLUMES	
FAULTED LOOP	388.4 FT^3
INTACT LOOPS (TOTAL)	868.5 FT^3

TABLE II-5

LARGE DRY CONTAINMENT PARAMETERS

Parameter	Value
Containment Volume	2.62 E+06 cubic ft
Initial Pressure	15.0 psia
Initial Temperature	120 degrees F
Fan Coolers Available	3
Fan Cooler Pressure Setpoint	7.9 psig
Fan Cooler Delay Time	35 seconds
Spray Flowrate	2600 GPM
Spray Pressure Setpoint	26.7 psig
Spray Delay Time	59 seconds

TABLE II-6

SUB-ATMOSPHERIC CONTAINMENT PARAMETERS

Parameter	Value
Containment Volume	2.26 E+06 cubic ft
Initial Pressure	9.11 psia
Initial Temperature	120 degrees F
Fan Coolers Available	0
Fan Cooler Pressure Setpoint	N/A
Fan Cooler Delay Time	N/A
Spray Flowrate	5000 GPM
Spray Pressure Setpoint	12.0 psig
Spray Delay Time	64 seconds

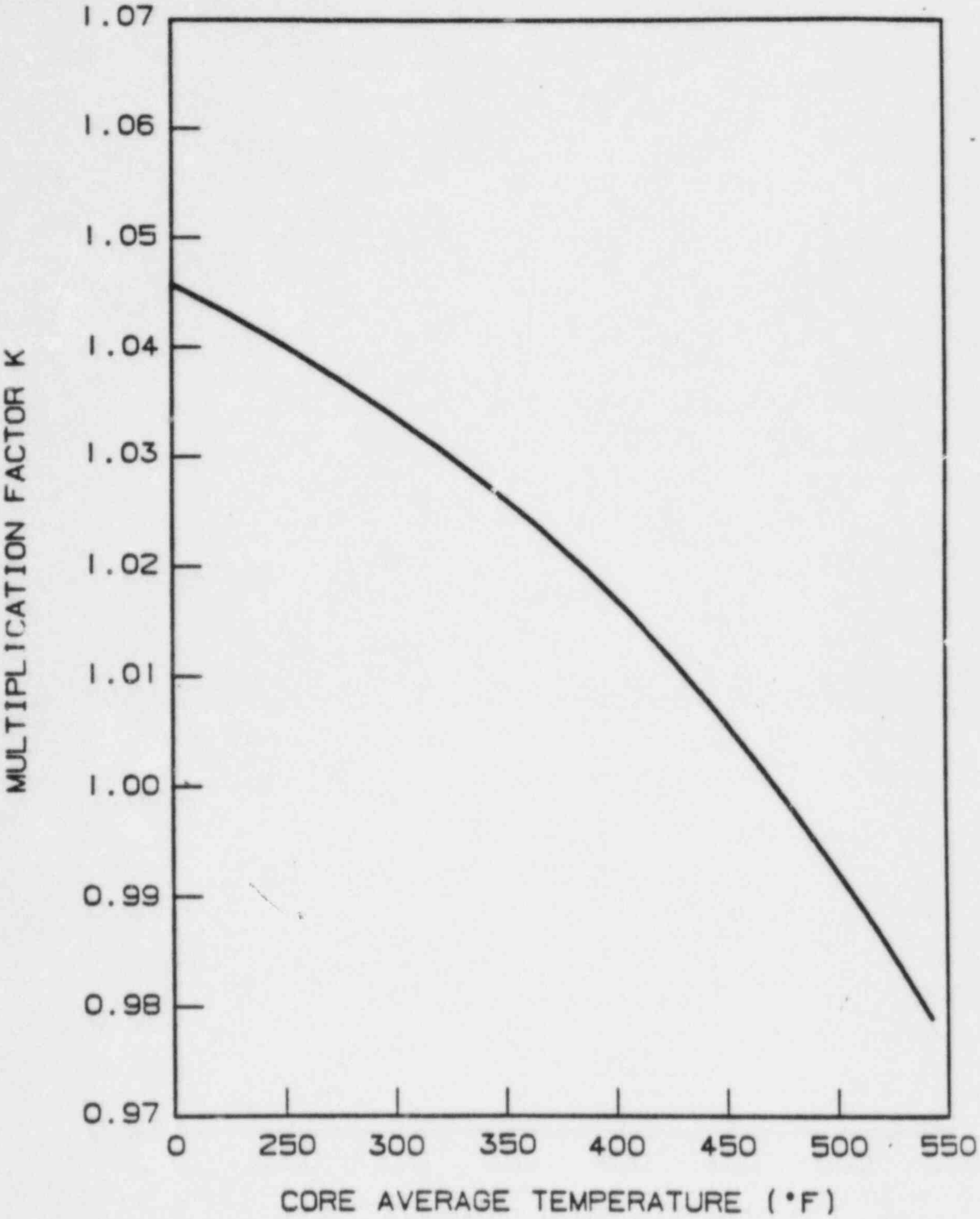

Figure II-1. Variation of Keff With Core Temperature

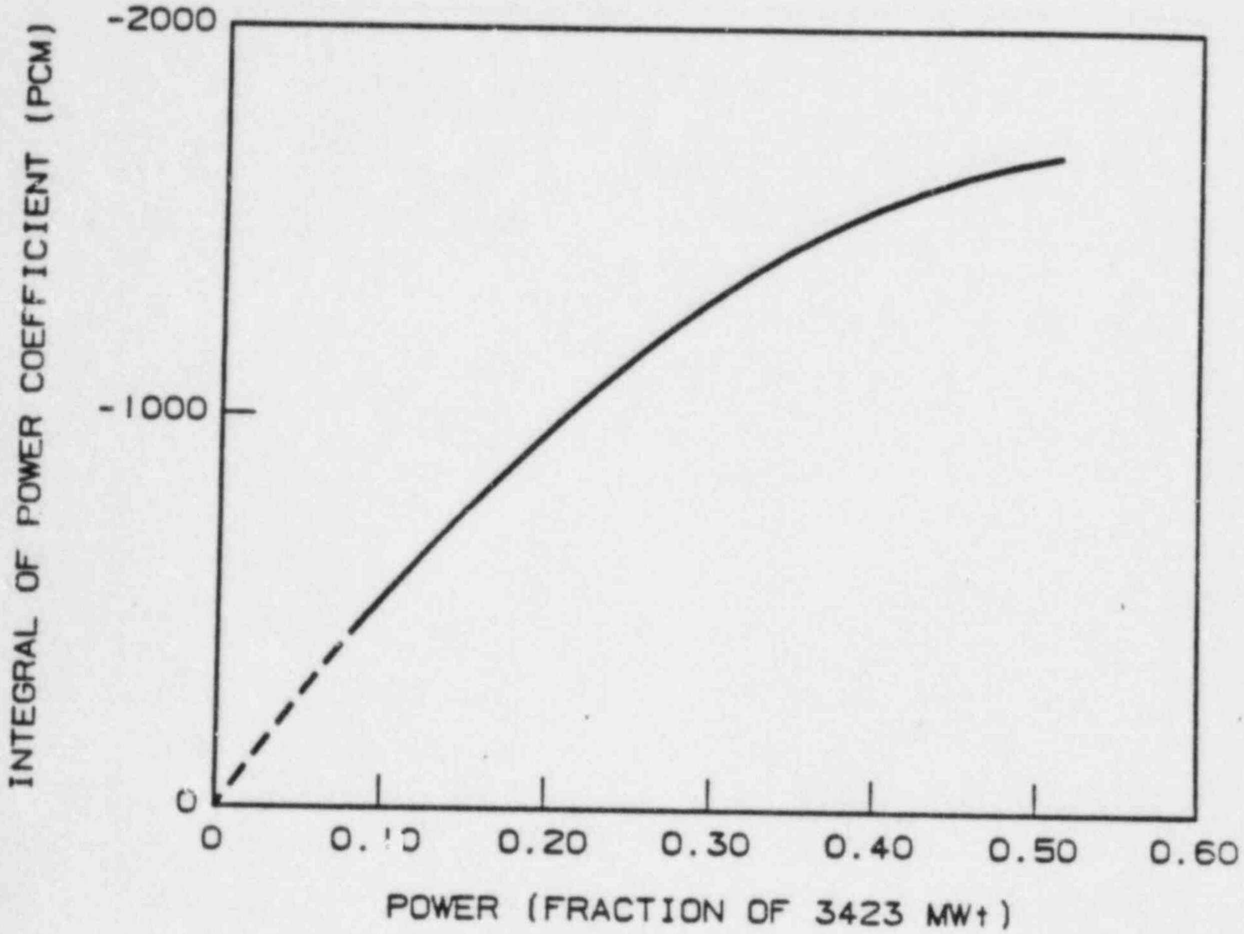

Figure II-2. Variation of Reactivity With Power at Constant Core Average Temperature

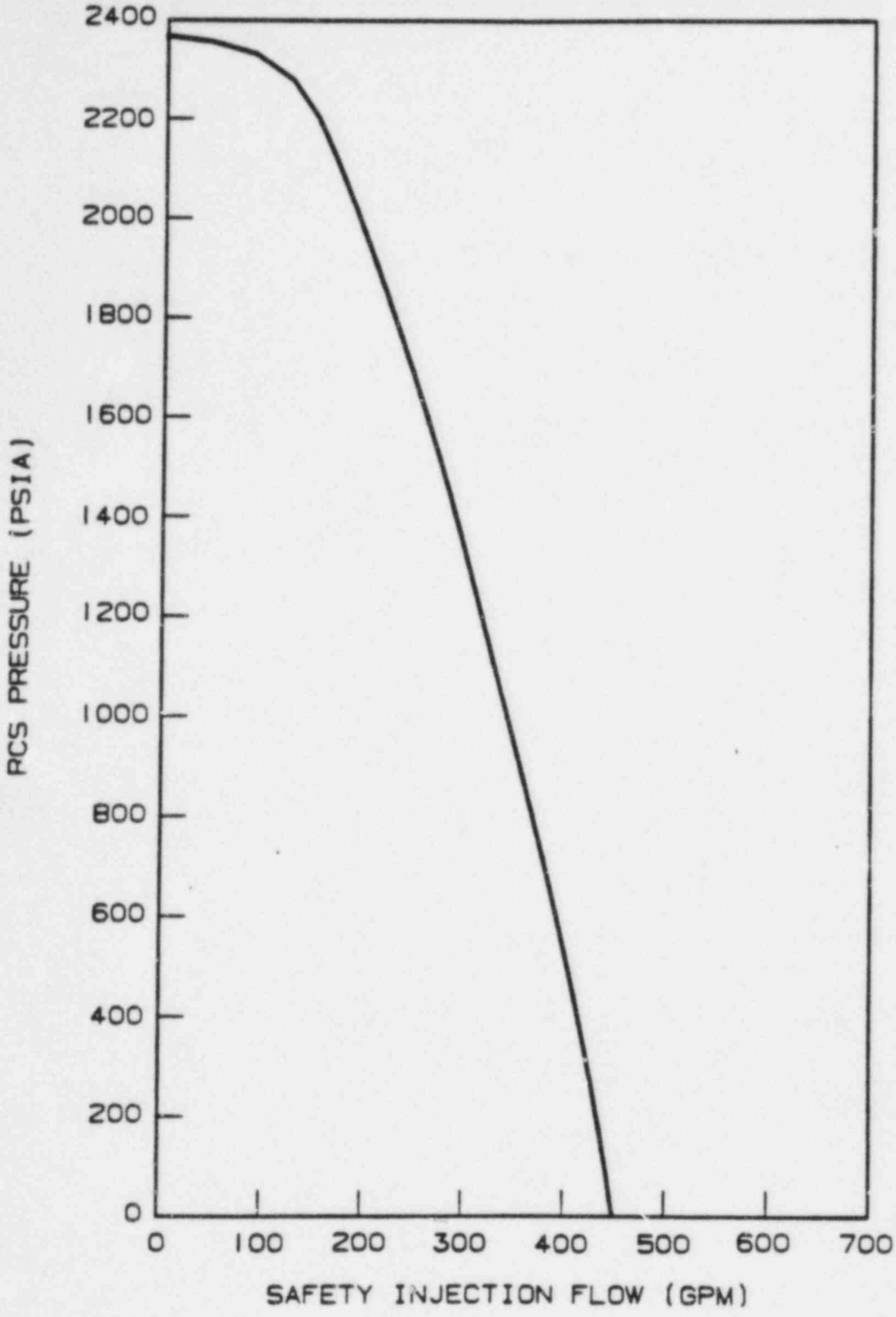

Figure II-3. Safety Injection Curve

III. MASS/ENERGY RELEASE BLOWDOWN ANALYSES

A. Introduction

To investigate the effects of steam superheating on mass and energy releases, and on containment pressure and temperature response, three sets of analyses were performed. The first set of analyses were performed assuming only saturated steam releases (i.e. no superheat) similar to analyses presented in Reference 1. These analyses were performed to provide a reference for subsequent analyses which account for steam superheating. The second set of analyses were performed in an identical manner as the first set with the exception that steam superheating, if predicted to occur, was calculated using the models described in Reference 6. The third set of analyses were performed to address the effect of various model assumptions and are described in Section III.D.

As dicussed in Section II. the steamline break mass and energy releases were generated using the LOFTRAN code. These releases were then input to the COCO containment code which models the containment pressure and temperature response to the releases.

B. Break Spectrum

Steamline breaks may be postulated to occur in any possible size, and at any plant power level. Depending upon the assumptions made, each of these parameters have competing effects on the resulting releases from the break. For example, increasing plant power increases the stored energy in the primary plant, and increases heat transfer into the steam generator. However, increasing plant power is generally accompanied by decreasing steam generator mass and steam pressure. The increased stored energy in the plant tends to increase the mass and energy release from a ruptured steam line, as well as the steam temperature resulting from steam superheating. Although the decreasing mass and pressure in the steam generator tend to reduce the mass and energy release, the reduced mass tends to result in earlier tube bundle uncovery and, therefore, earlier initiation of steam superheating.

The postulated break area can also have competing effects on blowdown results. Larger break areas will result in larger mass/energy release rates. Larger breaks however, will also result in earlier generation of protective trip signals following the break and thus a reduction in both the power production by the plant and the amount of high energy fluid available to be released to the containment.

The competing effects of break size and power level make a reasonable determination of the single, absolute "worst case", for the purpose of evaluating the impact of steam superheating, very difficult. To determine the impact of steam superheating on both containment temperature and pressure response following a steamline break, a spectrum of break sizes and power levels were investigated. This is the same approach which was taken in Reference 1 to address the impact of saturated mass/energy releases.

For the plant power levels of 102%, 70%, 30%, and 0% of nominal full load power, five break sizes were evaluated. These break sizes were chosen to be consistent with the break sizes analyzed in Reference 1. These break areas are:

1. A full double-ended rupture (DER) upstream of the flow measuring nozzle. For steam generator designs which do not have an integral flow restricting device, the maximum break area is determined by the area of the steam lines upstream of the flow measuring nozzles. A typical area of 4.6 ft^2 was used for the present analysis.

2. A full DER downstream of the flow measuring nozzle. For breaks which are postulated to occur downstream of the flow measuring nozzle, the maximum break area is limited by the area of the flow measuring device. A typical area of 1.4 ft^2 was used for the present analysis.

3. A small DER having an area just larger than that at which water entrainment occurs. These break areas at each power level were identified in Reference 1 as:

0.7 ft^2 @102% power
0.6 ft^2 @ 70% power
0.5 ft^2 @ 30% power
0.2 ft^2 @ 0% power

4. A small DER having an area just smaller than that at which entrainment occurs. These break areas at each power level were identified in Reference 1 as:

   0.6 ft^2 @102% power
   0.5 ft^2 @ 70% power
   0.4 ft^2 @ 30% power
   0.1 ft^2 @ 0% power

5. A small split rupture that will neither generate a steam line isolation signal from the Solid State Protection System (SSPS) nor result in water entrainment. These break areas at each power level were identified in Reference 1 as:

   0.215 ft^2/loop @ 102% power
   0.227 ft^2/loop @ 70% power
   0.236 ft^2/loop @ 30% power
   0.10 ft^2/loop @ 0% power

C. Mass/Energy Release Results

Large Double-Ended Ruptures

The LOFTRAN calculated mass and energy release results for the large double ended ruptures are summarized in Table III-1. As shown in the table, steam generator tube uncovery, and thus initiation of superheat, occurs [ ]a,c for the 4.6 ft^2 break and [ ]a,c for the 1.4 ft^2 ruptures. The results show that breaks initiated from full power operation result in [ ]a,c than the reduced power cases. This is due primarily to [ ]a,c

Figures III-1 through III-8 show a comparison of results with and without the calculation of superheat. As shown in the figures, break flow is [ ]^{a,c} After initiation of the break (time = 0), steam flow decreases rapidly due to the drop in steam pressure. As the tube bundle region begins to uncover, heat transfer from primary to secondary across the steam generator tubes in the uncovered tube region decreases. For the cases in which steam superheat is calculated, heat transfer switches from saturated liquid forced convection and film boiling to superheated steam forced convection as the tubes are uncovered. For the cases without superheat, no heat transfer is assumed in the uncovered tube region. Because superheated forced convection is a relatively ineffective mode of heat transfer in comparison with forced liquid convection and film boiling, there is an overall drop in heat transfer to the secondary side as the steam generator tubes uncover. This results in a further reduction in steam pressure and steam flow until a point of equilibrium between break flow and feedwater flow is reached.

Comparison of the effects of superheat on steam enthalpy and bre energy in Figures III-1 through III-8 shows that [ ]^{a,c}

Small Double-Ended and Split Ruptures

As shown in Table III-1, the calculations performed for the small double ended ruptures and split breaks [ ]^{a,c}

Containment Analysis Results

The results of the containment analyses are provided in Tables III-2 through III-5. Tables III-2 and III-3 provide a comparison of results with and without superheat for the large double ended ruptures. Table III-2 provides peak containment pressure and temperature results while Table III-3 shows the timing of tube bundle uncovery and spray actuation, as well as the timing of peak pressure and temperature.

As shown in Table III-2, the impact of superheat on peak containment pressure ranges from [ ]a,c The impact of superheat on peak temperature ranges from [ ]a,c For the [ ]a,c large break case (i.e., 1.4 ft^2 DER @ 0% power), the inclusion of superheat resulted in [ ]a,c

The results provided in Table III-3 show that superheat has [ ]a,c

The results shown in Table III-2 and III-3 indicate that [ ]a,c

Tables III-4 and III-5 show the results for all break sizes and power levels. In Table III-4 the results are sorted by peak pressure, while in Table III-5 the results are sorted by peak temperature. The results provided in these two tables show that [ ]a,c

D. Sensitivity Analyses

The assumptions and models used in the analyses presented in Section III.B are designed to result in a [ ]a,c of mass and energy releases. These assumptions have been shown to be conservative with respect to containment pressure and temperature response for saturated steam releases. Several of the assumptions, in particular the steam generator mass and feedwater assumptions, have the effect of [ ]a,c This is demonstrated to be the case for the small DER and split rupture cases presented in Section III.B.

In this section, sensitivity analyses are discussed which investigate the effect of the steam generator mass, feedwater, and tube uncovery assumptions on steamline break results. The analyses were performed to determine if [ ]^{a,c} of mass and energy releases continues to provide conservative results when the effects of steam superheating are included.

Two sets of sensitivity analyses, "predicted tube uncovery" and "early tube uncovery", are discussed below. The results from both sets of analyses are compared to results presented in Section III.B., "delayed tube uncovery".

<u>Predicted Tube Uncovery</u>

In the analyses presented in Section III.C, tube bundle uncovery is artificially delayed by requiring that the steam generator liquid mass be reduced to a small value before tube bundle uncovery is allowed to occur. Since, when tube bundle uncovery occurs, the heat transfer from the RCS to the secondary side decreases, delaying tube bundle uncovery tends to maximize the total energy released during a steam line break. The reduction in heat transfer which accompanies tube bundle uncovery allows steam pressure to decrease at a faster rate, thus the mass release rate decreases. Therefore, delaying tube bundle uncovery tends to keep steam generator pressure high and tends to maximize the mass release rate.

While delaying tube bundle uncovery tends to maximize mass and energy releases, the time at which steam superheating occurs is also delayed. To investigate this effect, analyses were performed in which a better estimate tube bundle uncovery time was modeled. Table III-6 shows a comparison of tube bundle uncovery times for the "delayed tube uncovery" cases and the "predicted tube uncovery" cases. The difference in tube bundle uncovery times range [.]^{a,c} Figures III-9 and III-10 show Break Flow, Break Enthalpy, and Break Energy Flow for two of the cases analyzed. These results are typical of the results which were obtained. As expected, the "predicted tube uncovery" cases result in a [

]^{a,c} The impact of the change in tube bundle uncovery time on peak containment pressure is shown in Table III-7. These results show that tube bundle uncovery time has [

]^{a,c} A comparison of calculated peak containment temperatures is shown in Table III-8. The results show that the impact of tube bundle uncovery time on [

]^{a,c}

Early Tube Uncovery

In addition to the analyses discussed above, sensitivity analyses were performed for which the model assumptions were changed so as to result in a maximization of steam superheating. This was accomplished by "forcing" an early tube bundle uncovery by assuming [

]^{a,c}

The combined effect of these assumptions results in [

]^{a,c} The effect on tube bundle uncovery times is shown in Table III-9. Figures III-11 through III-14 show Break Mass Flow, Break Enthalpy, and Break Energy Flow. As illustrated in the figures, the early tube uncovery cases result [

]^{a,c} The impact of early tube bundle uncovery on the peak containment pressure is shown in Table III-10. The "early tube uncovery" cases resulted in [ ]^{a,c}

Table III-11 shows containment peak temperature for the "delayed tube uncovery" and "early tube uncovery" cases. The impact of early tube bundle uncovery on peak temperature ranges [

]^{a,c}

Sub-atmospheric Containments

The containment analysis results presented in Table II-2 through III-5 are for a typical large dry containment building. However, the conclusions reached from these analyses are applicable to subatmospheric containments for the following reasons:

1. For subatmospheric plants, the containment spray setpoint would be reached much faster than in a large dry containment due to having a smaller containment and no containment fan coolers.

2. The spray flowrate for a subatmospheric containment is larger than in a large dry containment. This would tend to drive the containment atmosphere towards saturation.

To confirm this conclusion, mass and energy releases for a 1.4 ft^2 DER at 0% power were reanalyzed using typical subatmospheric containment parameters. Similar to the analyses presented in Section III.C, the calculations were performed both with steam superheat and without superheat for comparison.

Inclusion of steam superheat for these cases resulted in [ ]^{a,c} This compares with [ ]^{a,c} for the analyses performed using dry containment parameters (Table III-2). The case with superheat also resulted in [ ]^{a,c} This compares with [ ]^{a,c} for the analyses performed using dry containment parameters.

E. SUMMARY

The results presented in this report indicate that steam superheating has [ ]^{a,c} impact on peak containment temperature and pressure for dry and subatmospheric containment designs. The largest effect of steam superheating was seen for [

]a,c In all cases, however, the highest temperatures and pressures occurred for break sizes and power levels which [ ]a,c as shown in Tables III-4 and III-5. Therefore, the conclusions of current analyses based upon saturated steam releases are unchanged.

Sensitivity calculations were performed to confirm the conservatism of assumptions which [ ]a,c the total mass and energy releases, since these assumptions [ ]a,c the amount of steam superheating which would occur. The results of these sensitivity calculations demonstrate that containment temperatures and pressures are conservatively modeled by [ ]a,c the total mass and energy release, even when the effects of steam superheating are included.

In conclusion, the methodology described in WCAP-8822 (Reference 1) was found to conservatively predict mass and energy releases for dry and subatmospheric containments. The inclusion of steam superheating to this methodology was found to have [ ]a,c impact on peak temperature and pressure for dry and subatmospheric containments.

TABLE III-1

SUMMARY OF MASS/ENERGY RELEASE RESULTS

Break Description							
Break Size (FT2)	Break Type	Power Level (%NOM)	Break Quality (Dry/Wet)	Time of Tube Uncovery (Sec)	Peak Superheat Enthalpy (Btu/Lbm)	Time of Peak Enthalpy (Sec)	Break Energy Above Saturation (Btu/Lbm)

a,c

(1) - Tube bundle uncovery did not occur
NA - Not applicable

TABLE III-2

COMPARISON OF PEAK CONTAINMENT PRESSURE AND TEMPERATURE

Break Description				Peak Pressure (psig)			Peak Temp (F)		
Break Size (FT2)	Break Type	Power Level (%NOM)	Break Quality (Dry/Wet)	W/O SH	W/SH	Δ	W/O SH	W/SH	Δ

a,c

9127Q:1D/100485

TABLE III-3

COMPARISON OF TIME OF TUBE UNCOVERY WITH TIME OF PEAK TEMPERATURE AND PEAK PRESSURE

Break Description				Time of SG Tube Uncovery (Sec)	Time of Sprays Start (Sec)		Time of Peak Temp (Sec)		Time of Peak Pressure (Sec)	
Break Size (Ft2)	Break Type	Power Level (%NOM)	Break Quality (Dry/Wet)		W/O SH	W/SH	W/O SH	W/SH	W/O SH	W/SH

a,c

TABLE III-4

CONTAINMENT RESPONSE RESULTS, SORTED BY PEAK PRESSURE

Break Description				Peak Pressure (psig)		Peak Temp (F)		Comments
Break Size (FT2)	Break Type	Power Level (%NOM)	Break Quality (Dry/Wet)	W/O SH	W/SH	W/O SH	W/SH	

a,c

Key to Comments: 1 - Tube bundle uncovery did not occur

TABLE III-5

CONTAINMENT RESPONSE RESULTS, SORTED BY PEAK TEMPERATURE

Break Description				Peak Pressure (psig)		Peak Temp (F)		Comments
Break Size (FT2)	Break Type	Power Level (%NOM)	Break Quality (Dry/Wet)	W/O SH	W/SH	W/O SH	W/SH	

a,c

Key to Comments: 1 - Tube bundle uncovery did not occur

TABLE III-6

TUBE BUNDLE UNCOVERY TIME, "DELAYED TUBE UNCOVERY" VERSUS "PREDICTED TUBE UNCOVERY"

Break Description				Tube Bundle Uncovery Time (Sec)	
Break Size (FT2)	Break Type	Power Level (%NOM)	Break Quality (Dry/Wet)	Delayed Tube Uncovery	Predicted Tube Uncovery

a,c

(1) - Tube bundle uncovery not predicted

TABLE III-7

PEAK CONTAINMENT PRESSURE, "DELAYED TUBE UNCOVERY" VERSUS "PREDICTED TUBE UNCOVERY"

Break Description				Peak Pressure (psig)		
Break Size (FT2)	Break Type	Power Level (%NOM)	Break Quality (Dry/Wet)	Delayed Tube Uncovery W/SH	Predicted Tube Uncovery W/SH	Difference

a,c

(1) - Tube bundle uncovery not predicted,
Containment response analysis not performed.

TABLE III-8

PEAK CONTAINMENT TEMPERATURE, "DELAYED TUBE UNCOVERY" VERSUS "PREDICTED TUBE UNCOVERY"

Break Description				Peak Temperature (°F)		
Break Size (FT2)	Break Type	Power Level (%NOM)	Break Quality (Dry/Wet)	Delayed Tube Uncovery W/SH	Predicted Tube Uncovery W/SH	Difference

a,c

(1) - Tube bundle uncovery not predicted,
Containment response analysis not performed

TABLE III-9

TUBE BUNDLE UNCOVERY TIME, "DELAYED TUBE UNCOVERY" VERSUS "EARLY TUBE UNCOVERY"

Break Description				Tube Bundle Uncovery Time (Sec)	
Break Size (FT2)	Break Type	Power Level (%NOM)	Break Quality (Dry/Wet)	Delayed Tube Uncovery W/SH	Early Tube Uncovery W/SH

a,c

(1) - Tube bundle uncovery not predicted

TABLE III-10

PEAK CONTAINMENT PRESSURE, "DELAYED TUBE UNCOVERY" VERSUS "EARLY TUBE UNCOVERY"

Break Description				Peak Pressure (psig)		
Break Size (FT2)	Break Type	Power Level (%NOM)	Break Quality (Dry/Wet)	Delayed Tube Uncovery W/SH	Early Tube Uncovery W/SH	Difference

a,c

TABLE III-11

PEAK CONTAINMENT TEMPERATURE, "DELAYED TUBE UNCOVERY"
VERSUS "EARLY TUBE UNCOVERY"

Break Description				Peak Temperature (°F)		
Break Size (FT2)	Break Type	Power Level (%NOM)	Break Quality (Dry/Wet)	Delayed Tube Uncovery W/SH	Early Tube Uncovery W/SH	Difference

a,c

15027-4

a,c

Figure III-1. Break Mass Flow, Break Enthalpy, and Break Energy Flow, — 4.6 Ft^2 DER, — Hot Zero Power W/Entrainment

15027-5

a,c

Figure III-2. Break Mass Flow, Break Enthalpy, and Break Energy Flow, — 4.6 Ft^2 DER, — 30% Power W/Entrainment

15027-6

a,c

Figure III-3. Break Mass Flow, Break Enthalpy, and Break Energy Flow, — 4.6 Ft^2 DER, — 70% Power W/Entrainment

15027-7

a,c

Figure III-4. Break Mass Flow, Break Enthalpy, and Break Energy Flow, — 4.6 Ft^2 DER, — 102% Power W/Entrainment

15027-8

a,c

Figure III-5. Break Mass Flow, Break Enthalpy, and Break Energy Flow, — 1.4 Ft^2 DER, — Hot Zero Power W/Entrainment

15027-9

a,c

Figure III-6. Break Mass Flow, Break Enthalpy, and Break Energy Flow, — 1.4 Ft^2 DER, — 30% Power W/Entrainment

15027-10

a,c

Figure III-7. Break Mass Flow, Break Enthalpy, and Break Energy Flow, — 1.4 Ft^2 DER, — 70% Power W/Entrainment

15027-11

a,c

Figure III-8. Break Mass Flow, Break Enthalpy, and Break Energy Flow, — 1.4 Ft^2 DER, — 102% Power W/Entrainment

15027-13

a,c

Figure III-10. "Delayed Tube Uncovery" Versus "Predicted Tube Uncovery", Break Mass Flow, Break Enthalpy, and Break Energy Flow — Split Rupture, 30% Power

15027-12

a,c

Figure III-9. "Delayed Tube Uncovery" Versus "Predicted Tube Uncovery", Break Mass Flow, Break Enthalpy and Break Energy Flow — 1.4 Ft^2 DER, Hot Zero Power, W/Entrainment

15027-14

a,c

Figure III-11. "Delayed Tube Uncovery" Versus "Early Tube Uncovery", Break Mass Flow, Break Enthalpy, and Break Energy Flow — 1.4 Ft^2 DER, Hot Zero Power W/Entrainment

15027-15

a,c

Figure III-12. "Delayed Tube Uncovery" Versus "Early Tube Uncovery", Break Mass Flow, Break Enthalpy, and Break Energy Flow — Split Rupture, 30% Power

15027-16

a,c

Figure III-13. "Delayed Tube Uncovery" Versus "Early Tube Uncovery", Break Mass Flow, Break Enthalpy, and Break Energy Flow — Split Rupture, 70% Power

15027-17

a,c

Figure III-14. "Delayed Tube Uncovery" Versus "Early Tube Uncovery", Break Mass Flow, Break Enthalpy, and Break Energy Flow — Split Rupture, Hot Full Power

IV. REFERENCES:

1. Land, R. E., "Mass and Energy Releases Following a Steam Line Rupture", WCAP-8822 (Proprietary), and WCAP-8859 (Non-Proprietary) September 1976.

2. NS-EPR-2563, February 14, 1982, E. P. Rahe of Westinghouse to J. R. Miller, NRC, "Additional Information on WCAP-8822".

3. NS-CE-1694, February 13, 1978, C. Eicheldinger of Westinghouse to J. F. Stolz, NRC, "Additional Information on WCAP-8821 and WCAP-8822".

4. Hsieh, T., et. al., "Environmental Qualification Instrument Transmitter Temperature Transient Analysis", WCAP-8936, February 1977 (Proprietary), and WCAP-8937, February 1977 (Non-Proprietary).

5. Burnett, T. W. T., et. al., "LOFTRAN Code Description", WCAP-7907-P-A (Proprietary), WCAP-7907-A (Non-Proprietary).

6. Osborne, M. P., Love, D. S., "Mass and Energy Releases Following A Steam Line Rupture, Supplement 1 - Calculations of Steam Superheat in Mass/Energy Releases Following A Steamline Rupture", WCAP-8822-P-S1, January 1985.

7. Bordelon, E. T., et. al., "Containment Pressure Analysis Code (COCO)", WCAP-8326, July 1974.

FOR UNRESTRICTED DISTRIBUTION

DATE: ______________________________ WNES

Westinghouse Nuclear Energy Systems